Molecular Cell, Vol. 15, 367–374, August 13, 2004, Copyright ©2004 by Cell Press

Crystal Structure of Skp, a Prefoldin-like Chaperone that Protects Soluble and Membrane Proteins from Aggregation

Troy A. Walton and Marcelo C. Sousa*
Department of Chemistry and Biochemistry
University of Colorado at Boulder
Boulder, Colorado 80309

Summary

The Seventeen Kilodalton Protein (Skp) is a trimeric periplasmic chaperone that assists outer membrane proteins in their folding and insertion into membranes. Here we report the crystal structure of Skp from *E. coli*. The structure of the Skp trimer resembles a jellyfish with α-helical tentacles protruding from a β barrel body defining a central cavity. The architecture of Skp is unexpectedly similar to that of Prefoldin/GimC, a cytosolic chaperone present in eukaria and archea, that binds unfolded substrates in its central cavity. The ability of Skp to prevent the aggregation of model substrates in vitro is independent of ATP. Skp can interact directly with membrane lipids and lipopolysaccharide (LPS). These interactions are needed for efficient Skp-assisted folding of membrane proteins. We have identified a putative LPS binding site on the outer surface of Skp and propose a model for unfolded substrate binding.

Introduction

Outer membrane proteins (OMPs) from gram-negative bacteria are synthesized in the cytosol and translocated into the periplasm in an unfolded state (Danese and Silhavy, 1998; Driessen et al., 2001; Manting and Driessen, 2000). A chaperone system has been described in the periplasm that assists in the folding of OMPs and their insertion into the outer membrane (Danese and Silhavy, 1998; Missiakas et al., 1996; Missiakas and Raina, 1997). Members of this system include chaperones with peptidyl-prolyl isomerase activity (SurA, FkpA, RotA, and PpiD) and the Dsb protein-disulfide-isomerases. The protease DegP degrades the proteins that remain unfolded in the periplasm (Pallen and Wren, 1997).

An important player in this chaperone system is the Seventeen Kilodalton Protein (Skp, also known as OmpH and HlpA) (Hirvas et al., 1990; Koski et al., 1990; Missiakas et al., 1996). Skp has been characterized as a molecular chaperone that interacts with unfolded proteins as they emerge in the periplasm from the Sec translocation machinery (Harms et al., 2001; Schafer et al., 1999). Skp is required for efficient release of translocated proteins from the plasma membrane (Schafer et al., 1999). It is also important for the correct folding of several OMPs and their insertion into the outer membrane (Chen and Henning, 1996; De Cock et al., 1999). The knockout of the Skp gene in *E. coli* produced a phenotype with significantly reduced expression of OMPs in the outer membrane (Chen and Henning, 1996). In addition, the Skp knockout induced the σ^E response, increasing the transcription of the DegP protease (Missiakas and Raina, 1997). This suggests an accumulation of unfolded proteins in the periplasm of Skp deletion mutants (Schafer et al., 1999).

Skp interacts directly with the plasma membrane and with lipopolysaccharide (LPS), a specific glycolipid of the outer membrane of gram-negative bacteria (De Cock et al., 1999). The interaction with membranes alters Skp sensitivity to proteases, suggesting that the Skp conformation can be modulated by lipid binding (De Cock et al., 1999). Bulieris and coworkers have recently shown that Skp and LPS are required for the efficient folding and insertion into lipid bilayers of OmpA (a model β barrel OMP of *E. coli* extensively used to study membrane protein folding and insertion into membranes) (Bulieris et al., 2003). In addition, Skp has been shown to improve the folding of recombinant proteins targeted to the *E. coli* periplasm (Bothmann and Pluckthun, 1998).

Skp does not display sequence similarity to any other known chaperone, and the molecular mechanisms by which Skp carries out its chaperone function have remained undefined. Here we present the crystal structure of Skp from *E. coli*, which suggests a model for binding unfolded substrates. The architectural and functional similarities between Skp and Prefoldin, a cytosolic chaperone present in archea and eukarya, are also explored.

Results and Discussion

Structure Determination and Skp Model

The mature *E. coli* Skp (amino acids 21–161) was overexpressed as a His•Tag fusion and purified to homogeneity as described in Experimental Procedures. The His•Tag was cleaved with TEV protease, resulting in a mature Skp protein with a three additional amino acids (HGM) at the N terminus. The crystal structure of seleno-methionine Skp was solved using a three wavelength, 2.5 Å resolution MAD data set (Table 1). The final model was refined with data to 2.3 Å resolution (Table 1). The crystals contain three protomers per asymmetric unit and have a 68% solvent content. The protomers are arranged as a trimer, which is consistent with biochemical data suggesting that a trimer is the biologically active species (Schlapschy et al., 2004).

The Skp monomer is composed of two domains (Figure 1A). The small association domain (amino acids 19–41 and 133–161) folds into two short α helices and four β strands. This domain constitutes the limited hydrophobic core of Skp and mediates the oligomerization into trimers (Figure 1C). A second tentacle-shaped coiled α-helical domain is formed by amino acids 42 to 132. Significant conformational flexibility is apparent in the tentacle domain. The average B factor for all atoms in this domain is 68 Å^2, compared to 39 Å^2 for all atoms in the association domain. The experimental electron density was nevertheless unambiguous and allowed the complete modeling of the Skp monomer (chain C in the coordinate file).

*Correspondence: marcelo.sousa@colorado.edu

Table 1. Crystallographic Data and Phasing Statistics

Data Collection[a]

MAD Phasing	Wavelength (Å)	Resolution (Å)	% Complete	R_{sym}[b]	% > 3σ (I)	Average Redundancy
	λ1 = 0.9795 (edge)	25–2.50	99.6 (99.9)	0.061 (0.183)	88.6 (67.7)	6.6 (6.7)
	λ2 = 0.9794 (peak)	25–2.50	99.6 (99.9)	0.072 (0.201)	88.3 (66.7)	6.6 (6.7)
	λ3 = 0.9649 (remote)	25–2.50	99.6 (99.9)	0.060 (0.186)	88.3 (68.6)	6.6 (6.7)

Phasing

	Anomalous Diffraction Ratios[c]				Phasing Power				
Wavelength	λ1	λ2	λ3		+ Friedel Mate	− Friedel Mate			
λ1	0.074	0.037	0.048		1.23	2.31			
λ2		0.052	0.058		1.80	2.45			
λ3			0.051		reference	1.56			
Resolution (Å)	24.78–4.99	4.99–3.96	3.96–3.46	3.46–3.15	3.15–2.92	2.92–2.75	2.75–2.61	2.61–2.5	Overall
Figure-of-Merit	0.81	0.75	0.72	0.69	0.65	0.59	0.52	0.46	0.65

Refinement

Data	Wavelength (Å)	Resolution (Å)	% Complete	R_{sym}[b]	% > 3σ (I)	Average Redundancy
	0.9649	100–2.30 (2.38–2.30)	99.6 (99.9)	0.067 (0.301)	88.6 (67.7)	6.8 (6.7)
Model	R_{cryst}[e]	R_{free}	Protein atoms	Solvent atoms	Rmsd bonds (Å)	Rmsd Angles (°)
	0.232 (0.281)	0.259 (0.323)	2615	49	0.009	1.17

[a] Values in parentheses are for the highest resolution shell: 2.59–2.50 Å for the MAD phasing data sets.

[b] $R_{sym} = \Sigma_h\Sigma_i|I_i(h) - \langle I(h)\rangle|/\Sigma_h\Sigma_i I_i(h)$, where $I_i(h)$ is the I-th measurement of reflection h, and $\langle I(h)\rangle$ is the weighted mean of all measurements of h. Bijvoet measurements were treated as independent reflections for the MAD phasing data sets.

[c] Anomalous diffraction ratios = $\langle\Delta|F|\rangle/\langle|F|\rangle$, where $\langle\Delta|F|\rangle$ is the rms Bijvoet difference at a single wavelength (diagonal elements) or the rms dispersive difference between two wavelengths (off diagonal elements).

[d] Phasing Power = $\langle|F_H|\rangle/E$, where $\langle|F_H|\rangle$ is the rms structure factor amplitude for anomalous scatterers and E is the estimated lack of closure error. Phasing power is listed for each lack-of-closure expression between the reference data set (+Friedel mate at λ3) and the + or − Friedel set at each wavelength. Phasing powers were calculated using all data between 25.0 and 2.5 Å.

[e] $R_{cryst} = \Sigma|F_{obs} - F_{calc}|/\Sigma F_{obs}$, where F_{obs} = observed structure factor amplitude and F_{calc} = structure factor calculated from model. R_{free} is computed in the same manner as R_{cryst}, using the test set of reflections.

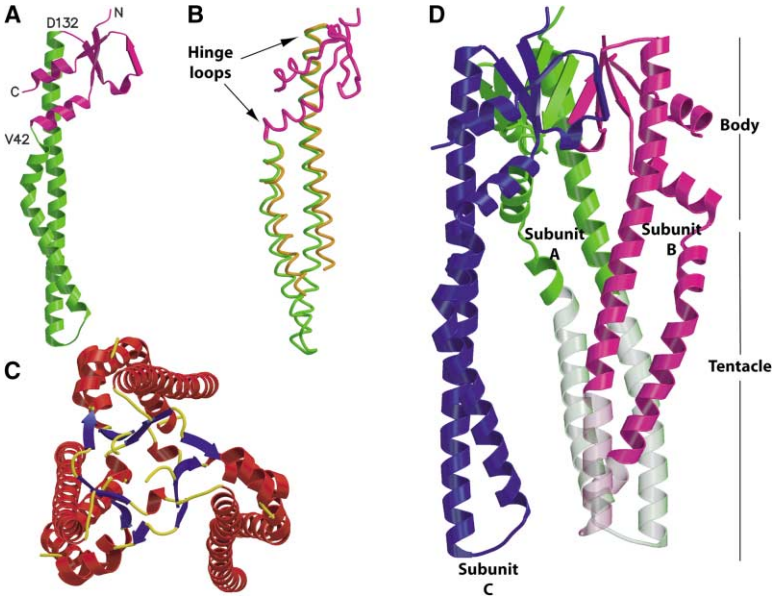

Figure 1. Crystal Structure of Skp

(A) Cartoon diagram of the Skp monomer. The body domain (amino acids 19–41, 133–161) is colored magenta and the tentacle domain (amino acids 42–132) is green.

(B) Superimposition of two Skp protomers. The body domain of both chains is magenta (rmsd 0.56 Å for all Cα atoms). The tentacle domain of chains B and C are gold and green, respectively.

(C) Top view of Skp trimer. β sheets forming a β barrel are blue and α helices are red.

(D) Side view of Skp trimer. Subunits A, B, and C are colored green, magenta, and blue, respectively. Semitransparent regions are not defined in the experimental density and were modeled by superimposing residues from chain C onto chains A and B as described in Experimental Procedures. All molecular figures were prepared with Molscript (Kraulis, 1991) and rendered with Raster3D (Merritt and Bacon, 1997).

Overall Structure of the Skp Trimer

The Skp trimer has a distinct quaternary structure similar in shape to a jellyfish (Figure 1D). The body consists of a tightly packed central β barrel surrounded by the C-terminal helices of the three subunits (Figure 1C). This gives the body a flat, triangular shape with ~44 Å sides and ~18 Å thickness. Each subunit contributes four β strands to the β barrel, which stabilizes the trimer and constitutes the limited hydrophobic core of the protein. Pointing away from the body are the three α-helical "tentacles" ~65 Å long that together with the body define a central cavity (Figure 2).

The three Skp subunits present in the asymmetric unit are related by a 3-fold rotation. The Cα of the body domains is well defined in all three protomers and superimpose with an rms deviation of 0.32 Å (A and C), 0.56 Å (B and C), and 0.53 Å (A and B). The structure of the tentacle domains of the Skp trimer is very flexible. When the body domains of protomers B and C are superimposed, the helices forming the tentacle domain diverge at amino acid 42 and converge again at amino acid 132 (Figure 1B). The loops connecting the body to the tentacles define hinge points that afford the tentacle domains considerable flexibility. A lattice contact stabilizes the conformation of the tentacle domain of chain C while no such contact exists for chains A and B. As a consequence, only broken electron density was seen for the areas in the tentacle domains corresponding to amino acids 68–90 in chain B and 48–104 in chain A and these residues could not be built into the density. However, for the purpose of analyzing the overall structure of the Skp trimer, those residues were modeled by superimposing chain C onto chains A and B (for details, see Experimental Procedures). The resulting model is shown in Figure 1D where the residues of the tentacle domains of subunits A and B for which no clear density is available are shown as semitransparent.

There are virtually no contacts between the tentacles,

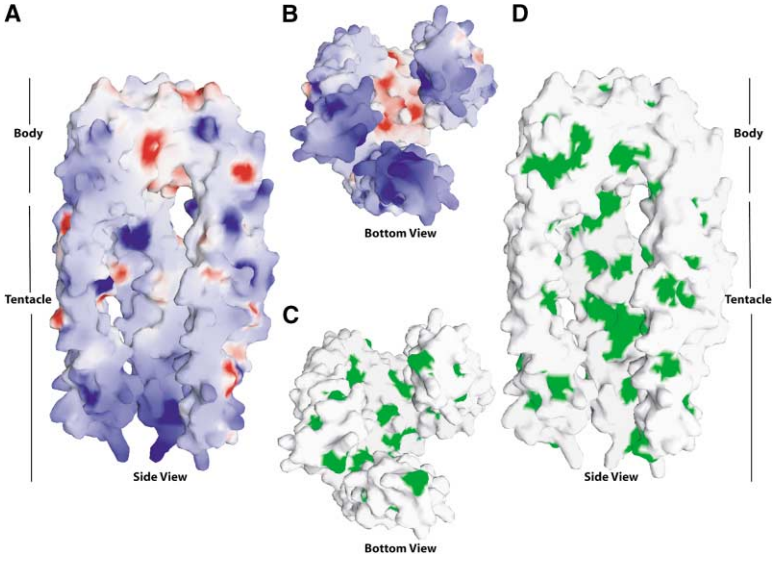

Figure 2. Skp Molecular Surface

(A and B) Two views of the electrostatic potential of the Skp trimer mapped to the molecular surface of Skp: (A) side view and (B) bottom view. Electrostatic potential mapped in red (negative) and blue (positive).

(C and D) The same views of the Skp trimer as in (A) and (B) but with hydrophobic residues (in green) mapped to the molecular surface. This model contains residues for chains A and B that were not defined in the experimental density and modeled by superimposing residues from chain C onto chains A and B as described in Experimental Procedures. Molecular surface renderings prepared using GRASP (Nicholls et al., 1991).

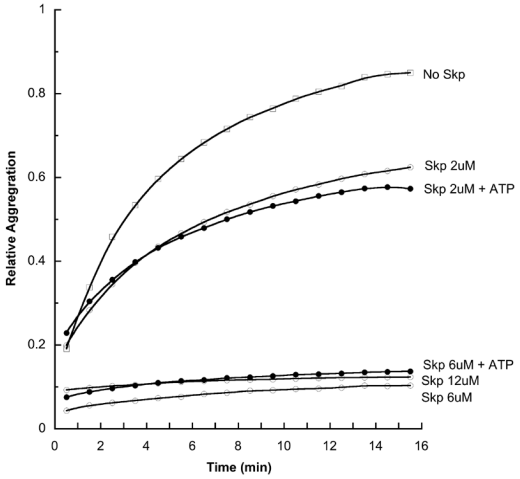

Figure 3. Chaperone Activity of Skp

Effect of Skp on the aggregation of lysozyme. Relative aggreation of 2 μM lysozyme, monitored at 360 nm, after dilution of denatured lysozyme into a solution containing buffer alone (open squares) or Skp in the concentrations indicated (open circles). Replicate experiments supplemented with 1 mM Mg^{2+}ATP are shown with closed circles.

and access to the cavity is open from the bottom and also from the sides where the tentacles are separated by ~25 Å. The electrostatic surface potential of Skp (Figure 2) reveals that the exterior face and the distal part of the tentacles are rich in positively charged residues (the calculated PI of Skp is 9.5). The interior of the cavity is less charged and contains patches of hydrophobic residues (Figures 2C and 2D). It is most likely that Skp binds its unfolded substrates in this central cavity. The volume of the cavity, approximated to a triangular prism (27 Å sides and 51 Å long), is ~33,000 $Å^3$. Assuming a folded protein occupies a volume of ~1.3 $Å^3$/Da (Xu et al., 1997), this cavity could accommodate a folded protein of ~25 kDa, assuming a perfect fit. However, unfolded proteins in a molten globule state are more loosely packed and would have to be smaller to fit in the cavity. OmpA, one of the best-characterized substrates of Skp, has a molecular mass of 18.8 kDa and would likely fit in the cavity in a molten globule state. Given that substrates bound in the cavity could protrude from the bottom and the sides, it is likely that Skp could accommodate substrates significantly bigger than OmpA. In addition, the flexibility of the tentacle domains we observe in the structure would allow Skp to tailor the size of the chamber to the size of the substrate.

The Chaperone Activity of Skp Is Independent of ATP

In vitro experiments have shown that the folding and insertion of OmpA into lipid bilayers is assisted by Skp (Bulieris et al., 2003). This chaperone activity of Skp did not require addition of ATP or any other nucleotide. In addition to OMPs, Skp can also prevent the aggregation of soluble proteins. Figure 3 shows that Skp is also able to effectively prevent the aggregation of a soluble protein like lysozyme as judged by the increase of absorbance at 360 nm. Skp prevented the aggregation of lysozyme almost completely at a Skp/lysozyme ratio of 3:1, consistent with the trimeric nature of Skp. This is consistent with reports that Skp improves the folding of recombinant proteins targeted to the periplasm in *E. coli* (Hayhurst and Harris, 1999). The addition of Mg•ATP had no effect on Skp activity (Figure 3). Moreover, Skp had no detectable ATPase activity either by itself or in the presence of denatured lysozyme (data not shown).

There is no consensus motif for ATP binding in the amino acid sequence of Skp, and no nucleotide binding site is apparent in its structure. Therefore, the available biochemical and structural data support the conclusion that Skp does not require ATP for its chaperone activity. This is in contrast to other molecular chaperones like the Hsp70 and Hsp60 families that have an intrinsic ATPase activity that is stimulated by binding of unfolded substrates. These proteins use the energy of ATP binding and hydrolysis to go through cycles of substrate binding and release (Hartl and Hayer-Hartl, 2002; Sigler et al., 1998). The ability to prevent protein aggregation in a nucleotide-independent fashion makes Skp functionally similar to Prefoldin (also known as GimC), a cytosolic chaperone present in eukarya and archea (Vainberg et al., 1998).

Skp Is a Prefoldin-like Protein

The overall shape of the Skp trimer bears a remarkable similarity with Prefoldin from the archaeum *Methanobacterium thermoautotrophicum* (mt) (Siegert et al., 2000). Although mtPrefoldin is a hexamer ($\alpha_2\beta_4$), for the purpose of comparing it to Skp, it can be thought of as a dimer of trimers. Like Skp, Prefoldin also has a "jellyfish" structure with a β barrel body and α-helical tentacles (Figure 4). They also share functional similarities. Skp prevents aggregation of proteins in the periplasm and delivers them to the outer membrane of gram-negative bacteria in an ATP-independent manner. Prefoldin prevents the aggregation of proteins in the cytosol and delivers them to class II cytosolic chaperonins (alternatively named c-cpn, CCT, or TriC), also in a nucleotide-independent fashion (Vainberg et al., 1998). In addition to preventing the aggregation of OMPs, Skp can, like Prefoldin, effectively prevent the aggregation of a soluble protein like lysozyme (Figure 3).

Electron microscopy (EM) reconstructions of Prefoldin bound to unfolded substrates have shown that the substrates occupy the central cavity and appear to bind the distal part of the tentacles (Lundin et al., 2004; Martin-Benito et al., 2002). This reinforces the notion that the unfolded substrates of Skp also bind in the central cavity. As shown in Figures 2A and 2B, the external surface of the Skp tentacles are rich in charged residues (particularly Lys and Arg), while the internal face lining the cavity is less charged and contains hydrophobic patches (Figures 2C and 2D).

In spite of these similarities, Skp and Prefoldin do not appear to share significant sequence similarity and have a circularly permutated structural topology. The N- and C-terminal sections of the Skp monomer form the body domain and the middle section forms the tentacle. In Prefoldin, the two helices that make up the tentacle are the N and C termini of the monomers, whereas the middle section of the protein constitutes the body.

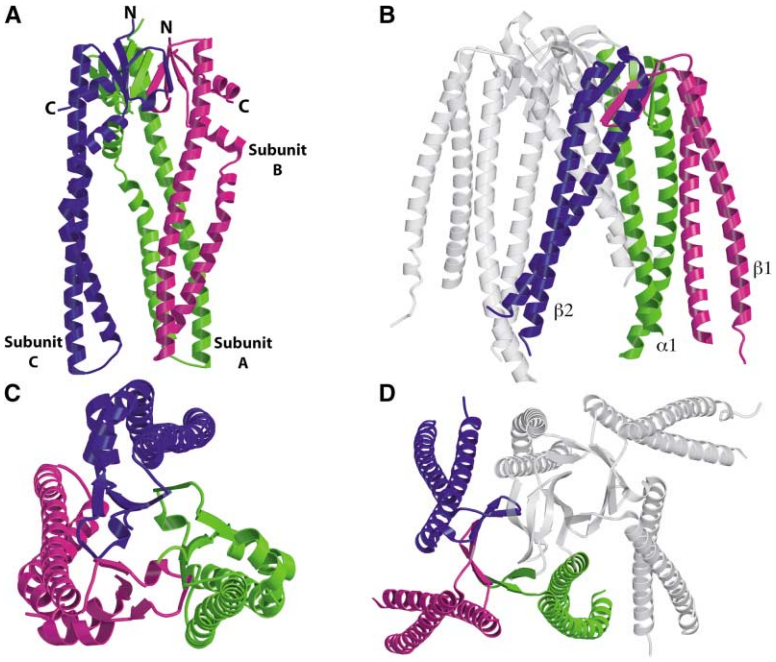

Figure 4. Structural Similarities between Skp and mtPrefoldin

(A) Ribbon diagram representing a side view of the Skp trimer. This model contains residues for chains A and B that were not defined in the experimental density and modeled by superimposing residues from chain C onto chains A and B as described in Experimental Procedures.

(B) Ribbon diagram representing side view of the prefoldin hexamer with two β subunits (blue and magenta) and one α subunit (green) colored while the rest of the molecule is transparent gray.

(C) Ribbon diagram representing the top view of the Skp trimer.

(D) Ribbon diagram representing the top view of the prefoldin hexamer colored as in (B).

Skp Contains a Putative Binding Site for Lipopolysaccharide

Skp is unique among chaperones in its ability to target membrane proteins and directly interact with lipids (De Cock et al., 1999). Skp and lipopolysaccharide (LPS) are required for the efficient folding and insertion of OmpA into lipid bilayers (Bulieris et al., 2003). The current hypothesis suggests that Skp interacts with OmpA as it emerges from the SecA/E/Y/G translocation machinery in the plasma membrane and prevents its aggregation (Harms et al., 2001; Schafer et al., 1999). After binding LPS, the Skp-OmpA complex delivers OmpA to the outer membrane where it inserts and folds (Bulieris et al., 2003).

Based on the crystal structure of FhuA (an outer membrane protein from *E. coli*) in complex with LPS, Ferguson and coworkers proposed a structural motif for LPS binding, consisting of four basic residues, that could be identified in other LPS binding proteins (Ferguson et al., 1998). Three of those four residues can be found in Skp in a similar spatial arrangement (rms deviation 1.75 Å for the Cα-Cγ atoms of K97, R107, and R108 in Skp matched to R382, K351, and K306 in FhuA, respectively). Skp has a glutamine (Q99) as opposed to a basic residue at the fourth position. In FhuA, that position is occupied by K439, which hydrogen bonds a phosphate oxygen in LPS, a function that could be served by Q99 in Skp. One additional residue that binds LPS in FhuA (E349) is also conserved in Skp (E49). Interestingly, a putative LPS binding site has been described in OmpT that also lacks one of the basic residues in the motif. Skp orthologs from other bacterial species display significant sequence variability (Figure 5B). It is striking that the residues we identify as forming a putative binding site for LPS are among the few that are strictly conserved. In addition, Q99 in Skp is in fact a basic residue in other species.

Based on this evidence, we propose that Skp contains a putative binding site for LPS. The site maps to the outer surface of the tentacle domain (Figure 5A). The overall positive charge of the tentacle surface may be important for the interaction of Skp with LPS and/or the negatively charged head groups of membrane phospholipids. Additional structural and biochemical studies of Skp with bound LPS will be needed to asses the importance of these residues in LPS binding.

A Working Model for Skp Function

Biochemical and structural data can be consolidated into a working model of how Skp assists in the folding and membrane insertion of OMPs (Figure 6). Studies of the translocation and folding of PhoE (an *E. coli* OMP) have shown that the protein interacts with Skp while it is being translocated across the cytosolic membrane by the Sec machinery (Harms et al., 2001). The aggregation of proteins once they are fully translocated into the periplasm is then prevented by their association with Skp. Skp would, like Prefoldin, sequester the unfolded substrate in the cavity formed by its tentacles. The structural flexibility displayed by the tentacle domains of Skp is likely important for its interaction with unfolded proteins of various sizes.

The efficient delivery of Skp-associated OmpA to lipid bilayers was shown to be dependent on LPS (Bulieris et al., 2003). We have identified a putative binding site for LPS in the external surface of the Skp tentacles. Previous studies have also provided biochemical evidence for a direct interaction between Skp and LPS. Interestingly, Skp was first purified as an LPS binding protein from *Salmonella minnesota* (Geyer et al., 1979). The binding of LPS to the Skp-OMP complex may be required to assist in folding and insertion of the membrane protein as proposed by Bulieris et al. (2003). Another possibility is that the Skp-OMP complex binds LPS embedded in the OM and this interaction mediates the docking and delivery of the membrane protein to the

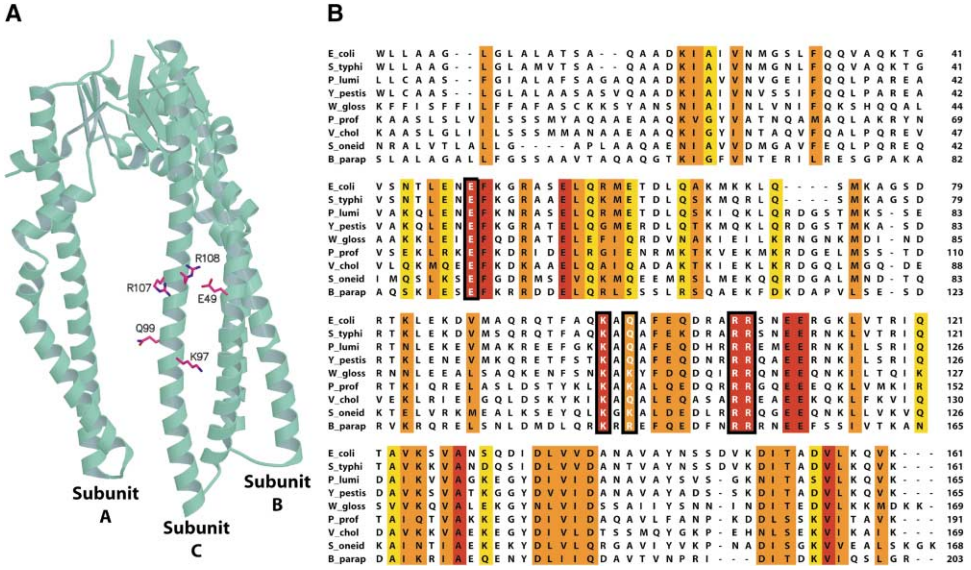

Figure 5. Putative LPS Binding Site in Skp

(A) Ribbon diagram of the Skp trimer in turquoise with putative LPS binding residues colored in magenta.

(B) Multiple sequence alignment of Skp protein sequences with a BLAST E-value of 1×10^{-5} or less. Strictly conserved residues are shaded in red while partially conserved residues are shaded orange and yellow. Residues proposed to bind LPS are boxed and highlighted in white. Abbreviation are as follows: E_coli, *Escherichia coli*; S_typhi, *Salmonella typhimurium*; P_lumi, *Photorhabdus luminescens*; Y_pestis, *Yersinia pestis*; W_gloss, *Wigglesworthia glossindia*; P_prof, *Photobacterium profundum*; V_chol, *Vibrio cholerae*; S_oneid, *Shewanella oneidensis*; B_parap, *Bordetella parapertussis*. Only free living organisms included. Only one representative Vibrio sequence is shown.

OM. A conformational change triggered by lipid binding may be responsible for the release of substrates into the membrane (De Cock et al., 1999). Once delivered to the outer membrane, OMPs would fold into their final conformation. Several studies have shown that OMPs can fold spontaneously when allowed to contact lipid bilayers or micelles before they aggregate (Kleinschmidt et al., 1999; Surrey et al., 1996). Skp has also been reported to improve the yield of functional proteins when they are overexpressed and targeted to the periplasm (Bothmann and Pluckthun, 1998; Hayhurst and Harris, 1999). Therefore, Skp may have an additional role in helping the folding of soluble periplasmic proteins, releasing them in the aqueous environment. Whether this activity also requires LPS is a question that requires further experimentation.

In summary, our model suggests that unfolded OMPs are sequestered in the cavity of Skp to prevent their aggregation and are delivered to the outer membrane for folding and insertion. The cycling of Skp between its free form and its Skp-OMP complex is modulated by LPS binding, not ATP. We have identified a putative LPS binding site in the structure of Skp. Detailed structure-function studies are now possible to refine this model and gain a better understanding of the chaperone-assisted folding and membrane insertion of membrane proteins.

Experimental Procedures

Protein Expression, Purification, and Crystallization

The Skp gene was PCR-amplified from genomic DNA of *E. coli* K12 using the primers forward 5′-AGGCATCCCGGGTTTAACCTGTTT CAGTACG-3′ and reverse 5′-CTTCTGCTCATATGGCTGACAAAATT GCAATCGTC-3′. Region 21–161 (SwissProt P11457) was cloned into a modified pET28 vector (pMS122) containing a TEV protease cleavage site downstream of the His_6 tag using XmaI and NdeI,

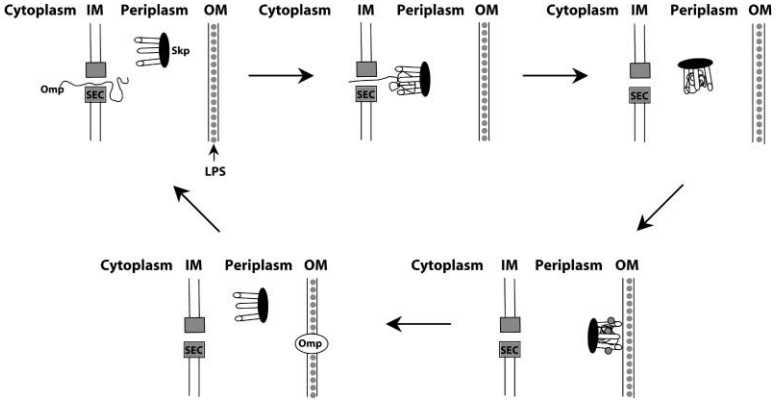

Figure 6. A Model for Skp Function

As proteins are translocated across the plasma membrane (inner membrane, IM) by the Sec translocation machinery (Sec), they are sequestered in the central cavity of Skp, which prevents their aggregation. Skp is then released from the plasma membrane and binds LPS. The Skp-OMP-LPS complex mediates the delivery and insertion of OMPs into the outer membrane (OM). The OMP is released into the membrane where it folds to its native conformation. Skp is now free to restart the cycle.

yielding a protein with an N-terminal His_6 tag followed by a TEV protease cleavage site. This plasmid was used to express protein in *E. coli* Rosetta cells. Cells were grown at 37°C in Luria-Bertrani (LB) media supplemented with 50 mg/l kanamycin to a cell density corresponding to A_{600} ~0.6. Skp expression was induced by addition of 0.4 mM isopropyl-B-D-thio-galactoside (IPTG) and cells were grown for an additional 4 hr at 37°C before harvesting by centrifugation. The pellet was resuspended in buffer A (25 mM HEPES [pH 7.5], 250 mM NaCl) supplemented with 0.5 mg/ml lysozyme and either frozen or processed immediately as follows. Cells were lysed by sonication and centrifuged at 17,500 rpm in a JA20 rotor for 30 min. The supernatant was applied to a Ni-NTA column equilibrated in buffer A. The column was washed extensively (25 column volumes) with wash buffer (buffer A plus 25 mM imidazole). Protein was eluted in approximately 80 ml of elution buffer (buffer A plus 300 mM imidazole). The eluate was dialyzed back into buffer A for the TEV cleavage reaction. TEV was added at a 1:10 (w/w) ratio to the Skp protein solution supplemented with 10 mM DTT and allowed to incubate at room temperature for 48 hr. This mixture was applied to a Superdex200 column running in buffer A, and fractions containing pure Skp were pooled and concentrated for crystallization trials. The final yield was approximately 30 mg per liter of culture. Selenomethionine (SeMet)-labeled protein was prepared by growing 4 l of Rosetta cells at 37°C in minimal media containing M9 salts, 2 mM $MgSO_4$, 0.1 mM $CaCl_2$, 0.4% glucose, and 50 μg/ml kanamycin to an OD_{600} ~0.6. Cultures were then supplemented with 100 μg/ml D-lys, D-Phe, and D-Thr, 50 μg/ml D-Ile and D-Val, and 60 μg/ml SeMet and grown for an additional 20 min before addition of 0.4 mM IPTG. Again, cells were grown for an additional 4 hr at 37°C before harvesting by centrifugation, and Se-Met Skp was purified as described above. Se-Met Skp crystals were grown in hanging drops from 35% PEG 350 monomethy ether, 85 mM $NH_4H_2PO_4$, and 0.1 M Tris (pH 8.5) and a stock of Skp at a concentration of 16.9 mg/ml. Crystals had approximate dimensions of 50 × 100 × 500 μm and grew at 4°C in 48–72 hr after tray set-up at room temperature. Prior to data collection, crystals were cryo-protected in a solution containing mother liquor supplemented with 15% glucose.

Data Collection, Structure Determination, and Refinement

Multiwavelength anomalous scattering data were measured at three wavelengths with an inverse beam strategy from a frozen crystal of SeMet-Skp using a Quantum-4 CCD detector (Area Detector Systems Corporation) at beamline 8.2.1 of the Advanced Light Source (Lawrence Berkeley National Laboratory). The crystal belongs to space group $P2_12_12_1$ with unit cell dimensions a = 55.83 Å, b = 84.19 Å, c = 160.18 Å, and three Skp protomers per asymmetric unit. All data were processed and scaled using the DENZO/SCALEPACK program package (Otwinowski and Minor, 1997). Data collection statistics for the SeMet-Skp are summarized in Table 1.

The program Solve (http://www.solve.lanl.gov/; Terwilliger, 2004) was used to calculate an anomalous difference Patterson map using data collected at the absorption peak wavelength of the SeMet-Skp crystal in the 25–2.5 Å resolution range. Solve's automated Patterson search identified nine selenium sites (out of a potential 18) and the 3-fold noncrystallographic symmetry operation that related them (Terwilliger, 2002b). These nine sites were used to calculate initial phases using the Philips-Hodgson method and maximum likelihood refinement as implemented in the program CNS (Brunger et al., 1998). MAD phasing statistics are summarized in Table 1. The phases were then modified by solvent flipping and histogram matching as implemented in CNS. The resulting electron density map was readily interpretable and automated model building was performed using the program Resolve (Terwilliger, 2002a, 2002c, 2004). Partial models were built automatically for all three subunits of Skp and manual model building assisted by the program O (Jones, 1978) to complete the model.

Refinement of the SeMet-Skp model was carried out using the program CNS using data from the remote wavelength in the 25–2.3 Å resolution range. Before refinement, a subset of the data was selected as a test set for crossvalidation. An overall anisotropic temperature factor correction was used throughout refinement. The initial SeMet-Skp model was subjected to a round of slow-cool torsional annealing followed by positional refinement and group B factor refinement using the MLHL target function and the solvent-flipped phases as restraints. Manual rebuilding and several rounds of simulated annealing and positional and atomic B factor refinement were then carried out until no further drop in the R factors was observed. At this stage, several solvent molecules were clearly visible and added to the model. A new round of refinement using the MLHL target function was carried out followed by a round of refinement using the MLF target and no phase restraints. Manual rebuilding interspersed with positional and B factor refinement continued until no further improvement of the free R factor was observed. The final model contains all residues for chain C (19–161), residues 23–67 and 91–161 for chain B, residues 19–47 and 105–161 for chain A, and 49 water molecules. The amino acids that are missing from our model (68–90 in chain B and 48–104 in chain A) make the R factors (R_{crys} = 23.1 and R_{free} = 25.9) slightly higher than would be expected for a structure at this resolution because they cannot be modeled but still contribute to the observed structure factor amplitudes.

For the purpose of analyzing the overall structure of the Skp trimer, we constructed a spliced model. We superimposed amino acids 42–132 from the tentacle domain of chain C on the partial models of chains A and B (rmsd = 0.12 Å and 0.43 Å, respectively) and spliced the missing residues to make a complete trimer (Figure 1). The spliced tentacle domains for chains A and B coincided with the broken electron density we observed in the experimental maps. However, attempts to further refine the structure with these residues did not improve the R_{free} value. Therefore, residues 68–90 in chain B and residues 48–104 in chain A are not included in the coordinate file and were modeled based on the structure of the fully defined chain C only for the purpose of analyzing the overall structure of the Skp homotrimer.

Aggregation Assay

Assays were carried out as described (Lundin et al., 2004). Hen egg-white lysozyme (Sigma) was dissolved in denaturing buffer (6 M guanidine HCl, 250 mM NaCl, 25 mM HEPES [pH 7.5], 50 mM DTT) and then diluted 100× to a final concentration of 2 μM into buffer A alone or containing various concentrations of Skp or Skp plus 1 mM Mg^{2+}ATP. Aggregation of lysozyme was monitored at A_{360} for 15 min at room temperature. Raw absorbance data was normalized and relative aggregation was defined as a fraction of the final absorbance in the no-Skp control.

Acknowledgments

We thank Sandra I. Metzner for excellent technical assistance in biochemistry. We are indebted to Gerry McDermott, Corie Ralston, J.J. Plecs, and the staff at the ALS for assistance in collecting crystallographic data. This work is based upon research carried out at the Advanced Light Source, which is funded by the Department of Energy. This work is supported in part by a grant from the William M. Keck Foundation.

Received: June 24, 2004
Revised: July 19, 2004
Accepted: July 21, 2004
Published: August 12, 2004

References

Bothmann, H., and Pluckthun, A. (1998). Selection for a periplasmic factor improving phage display and functional periplasmic expression. Nat. Biotechnol. *16*, 376–380.

Brunger, A.T., Adams, P.D., Clore, G.M., DeLano, W.L., Gros, P., Grosse-Kunstleve, R.W., Jiang, J.S., Kuszewski, J., Nilges, M., Pannu, N.S., et al. (1998). Crystallography & NMR system: a new software suite for macromolecular structure determination. Acta Crystallogr. D Biol. Crystallogr. *54*, 905–921.

Bulieris, P.V., Behrens, S., Holst, O., and Kleinschmidt, J.H. (2003). Folding and insertion of the outer membrane protein OmpA is assisted by the chaperone Skp and by lipopolysaccharide. J. Biol. Chem. *278*, 9092–9099.

Chen, R., and Henning, U. (1996). A periplasmic protein (Skp) of

Escherichia coli selectively binds a class of outer membrane proteins. Mol. Microbiol. *19*, 1287–1294.

Danese, P.N., and Silhavy, T.J. (1998). Targeting and assembly of periplasmic and outer-membrane proteins in *Escherichia coli*. Annu. Rev. Genet. *32*, 59–94.

De Cock, H., Schafer, U., Potgeter, M., Demel, R., Muller, M., and Tommassen, J. (1999). Affinity of the periplasmic chaperone Skp of *Escherichia coli* for phospholipids, lipopolysaccharides and non-native outer membrane proteins. Role of Skp in the biogenesis of outer membrane protein. Eur. J. Biochem. *259*, 96–103.

Driessen, A.J., Manting, E.H., and van der Does, C. (2001). The structural basis of protein targeting and translocation in bacteria. Nat. Struct. Biol. *8*, 492–498.

Ferguson, A.D., Hofmann, E., Coulton, J.W., Diederichs, K., and Welte, W. (1998). Siderophore-mediated iron transport: crystal structure of FhuA with bound lipopolysaccharide. Science *282*, 2215–2220.

Geyer, R., Galanos, C., Westphal, O., and Golecki, J.R. (1979). A lipopolysaccharide-binding cell-surface protein from *Salmonella minnesota*. Isolation, partial characterization and occurrence in different Enterobacteriaceae. Eur. J. Biochem. *98*, 27–38.

Harms, N., Koningstein, G., Dontje, W., Muller, M., Oudega, B., Luirink, J., and de Cock, H. (2001). The early interaction of the outer membrane protein phoe with the periplasmic chaperone Skp occurs at the cytoplasmic membrane. J. Biol. Chem. *276*, 18804–18811.

Hartl, F.U., and Hayer-Hartl, M. (2002). Molecular chaperones in the cytosol: from nascent chain to folded protein. Science *295*, 1852–1858.

Hayhurst, A., and Harris, W.J. (1999). *Escherichia coli* skp chaperone coexpression improves solubility and phage display of single-chain antibody fragments. Protein Expr. Purif. *15*, 336–343.

Hirvas, L., Coleman, J., Koski, P., and Vaara, M. (1990). Bacterial 'histone-like protein I' (HLP-I) is an outer membrane constituent? FEBS Lett. *262*, 123–126.

Jones, A. (1978). A graphics model building and refinement system for macromolecules. J. Appl. Crystallogr. *11*, 268–272.

Kleinschmidt, J.H., Wiener, M.C., and Tamm, L.K. (1999). Outer membrane protein A of *E. coli* folds into detergent micelles, but not in the presence of monomeric detergent. Protein Sci. *8*, 2065–2071.

Koski, P., Hirvas, L., and Vaara, M. (1990). Complete sequence of the ompH gene encoding the 16-kDa cationic outer membrane protein of *Salmonella typhimurium*. Gene *88*, 117–120.

Kraulis, P. (1991). MOLSCRIPT: a program to produce both detailed and schematic plots of protein structures. J. Appl. Crystallogr. *24*, 946–950.

Lundin, V.F., Stirling, P.C., Gomez-Reino, J., Mwenifumbo, J.C., Obst, J.M., Valpuesta, J.M., and Leroux, M.R. (2004). Molecular clamp mechanism of substrate binding by hydrophobic coiled-coil residues of the archaeal chaperone prefoldin. Proc. Natl. Acad. Sci. USA *101*, 4367–4372.

Manting, E.H., and Driessen, A.J. (2000). *Escherichia coli* translocase: the unravelling of a molecular machine. Mol. Microbiol. *37*, 226–238.

Martin-Benito, J., Boskovic, J., Gomez-Puertas, P., Carrascosa, J.L., Simons, C.T., Lewis, S.A., Bartolini, F., Cowan, N.J., and Valpuesta, J.M. (2002). Structure of eukaryotic prefoldin and of its complexes with unfolded actin and the cytosolic chaperonin CCT. EMBO J. *21*, 6377–6386.

Merritt, E.A., and Bacon, D.J. (1997). Raster3D: photorealistic molecular graphics. Methods Enzymol. *277*, 505–524.

Missiakas, D., and Raina, S. (1997). Protein folding in the bacterial periplasm. J. Bacteriol. *179*, 2465–2471.

Missiakas, D., Betton, J.M., and Raina, S. (1996). New components of protein folding in extracytoplasmic compartments of *Escherichia coli* SurA, FkpA and Skp/OmpH. Mol. Microbiol. *21*, 871–884.

Nicholls, A., Sharp, K.A., and Honig, B. (1991). Protein folding and association: insights from the interfacial and thermodynamic properties of hydrocarbons. Proteins *11*, 281–296.

Otwinowski, Z., and Minor, W. (1997). Processing of X-ray diffraction data collected in oscillation mode. Methods Enzymol. *276*, 307–326.

Pallen, M.J., and Wren, B.W. (1997). The HtrA family of serine proteases. Mol. Microbiol. *26*, 209–221.

Schafer, U., Beck, K., and Muller, M. (1999). Skp, a molecular chaperone of gram-negative bacteria, is required for the formation of soluble periplasmic intermediates of outer membrane proteins. J. Biol. Chem. *274*, 24567–24574.

Schlapschy, M., Dommel, M.K., Hadian, K., Fogarasi, M., Korndorfer, I.P., and Skerra, A. (2004). The periplasmic *E. coli* chaperone Skp is a trimer in solution: biophysical and preliminary crystallographic characterization. Biol. Chem. *385*, 137–143.

Siegert, R., Leroux, M.R., Scheufler, C., Hartl, F.U., and Moarefi, I. (2000). Structure of the molecular chaperone prefoldin: unique interaction of multiple coiled coil tentacles with unfolded proteins. Cell *103*, 621–632.

Sigler, P.B., Xu, Z., Rye, H.S., Burston, S.G., Fenton, W.A., and Horwich, A.L. (1998). Structure and function in GroEL-mediated protein folding. Annu. Rev. Biochem. *67*, 581–608.

Surrey, T., Schmid, A., and Jahnig, F. (1996). Folding and membrane insertion of the trimeric beta-barrel protein OmpF. Biochemistry *35*, 2283–2288.

Terwilliger, T.C. (2002a). Automated structure solution, density modification and model building. Acta Crystallogr. D *58*, 1937–1940.

Terwilliger, T.C. (2002b). Rapid automatic NCS identification using heavy-atom substructures. Acta Crystallogr. D *58*, 2213–2215.

Terwilliger, T.C. (2002c). Statistical density modification with non-crystallographic symmetry. Acta Crystallogr. D *58*, 2082–2086.

Terwilliger, T. (2004). SOLVE and RESOLVE: automated structure solution, density modification and model building. J. Synchrotron Radiat. *11*, 49–52.

Vainberg, I.E., Lewis, S.A., Rommelaere, H., Ampe, C., Vandekerckhove, J., Klein, H.L., and Cowan, N.J. (1998). Prefoldin, a chaperone that delivers unfolded proteins to cytosolic chaperonin. Cell *93*, 863–873.

Xu, Z., Horwich, A.L., and Sigler, P.B. (1997). The crystal structure of the asymmetric GroEL-GroES-(ADP)7 chaperonin complex. Nature *388*, 741–750.

Accession Numbers

The coordinates of the structure of Skp and the corresponding structure factors have been deposited in the Protein Data Bank under accession number 1U2M.